

## Article

# Adsorption and Structuration of PEG Thin Films: Influence of the Substrate Chemistry

Maurice Brogly \* , Sophie Bistac and Diane Bindel

Laboratoire de Photochimie et d'Ingénierie Macromoléculaires, Université de Haute Alsace, 3b Rue Alfred Werner, 68093 Mulhouse, France

\* Correspondence: maurice.brogly@uha.fr

**Abstract:** This study investigates polyethylene glycol (PEG) homopolymer thin film adsorption on gold surfaces of controlled surface chemistry. The conformational states of physisorbed PEG are analyzed through polarization modulation infrared reflection–absorption spectrometry (PM-IRRAS). The PM-IRRAS principle is based on specific optical selection rules allowing the detection of surface-specific FTIR response of thin polymer films on the basis of differential reflectivity at the polymer/substrate interface for p- and s-polarized light. The intensification of the electric field generated at the PEG/substrate interface for p-polarized IR light in comparison with s-polarized light permits the analysis of PEG chain anisotropy and conformational changes induced by the adsorption. Results showed that PEG adsorbs on model substrates having a rather hydrophilic character in a way that the PEG chains spread parallel to the surface. In the case of a very hydrophilic substrate, the adsorbed PEG chains are in a stable thermodynamic state which allows them to arrange and crystallize as stacked crystalline lamellae after adsorption. The surface topography and morphology of the PEG thin films were also investigated by atomic force microscopy (AFM). While in the bulk state, PEG crystallizes in the form of large spherulites; on substrates whose adsorption is favored by surface chemistry, PEG crystallizes in the form of stacked lamellae with a thickness equal to 20 nm. Conversely, on a hydrophobic substrate, the PEG chains do not crystallize and adsorption occurs in the statistical coil state.



**Citation:** Brogly, M.; Bistac, S.; Bindel, D. Adsorption and Structuration of PEG Thin Films: Influence of the Substrate Chemistry. *Polymers* **2024**, *16*, 1244. <https://doi.org/10.3390/polym16091244>

Academic Editors: Javier Esteban Durantini and Daniel A. Heredia

Received: 29 March 2024  
Revised: 25 April 2024  
Accepted: 26 April 2024  
Published: 29 April 2024



**Copyright:** © 2024 by the authors. Licensee MDPI, Basel, Switzerland. This article is an open access article distributed under the terms and conditions of the Creative Commons Attribution (CC BY) license (<https://creativecommons.org/licenses/by/4.0/>).

**Keywords:** polyethylene glycol (PEG); thin film; surface chemistry; PM-IRRAS spectrometry; structuration

## 1. Introduction

Polyethylene glycol (PEG) is a biocompatible semi-crystalline polymer with hydrophilic behavior that can be synthesized by anionic, cationic or opening polymerization of an ethylene glycol monomer. PEG is used in the composition of a large number of industrial products, such as binders and bases in cosmetic formulations, plasticizers in adhesives, detergents in household products due to their solubility in water and low toxicity, or as a co-solvent of water, as it reduces solution polarity to favor the solubility of organic molecules. PEG is thus a polymer of great interest for various applications, particularly in the field of biotechnology. Indeed, being biocompatible and non-toxic, PEG does not damage proteins or biological cells. Its hydrophilic character allows it to repel other polymers in aqueous solution [1], which makes it a very good candidate as an encapsulating agent [2]. This property is exploited by Pean et al. [3] to stabilize a protein during the encapsulation process by using PEG with a 400 g.mol<sup>-1</sup> molar mass. The hydrophilicity of PEG also allowed Albertsson [4] to discover that a mixture of PEG and dextran forms a two-phase polymer system, allowing the purification of biological compounds [4]. In addition to not damaging biological cells, PEG can interact with cell membranes to trigger cell fusion, which is a key process in the field of biotechnology [5,6]. PEGs with molar masses varying between 200 g.mol<sup>-1</sup> and 20,000 g.mol<sup>-1</sup> allow access to even more varied properties in the biomedical field when they bind covalently with

proteins. Buchowski et al. showed that attachment by covalent bonding of PEG to proteins increases the lifetime of biological serums [7]. Mori et al. demonstrated that the attachment by covalent bonding of PEG to a surface considerably delays the adsorption of proteins on these surfaces [8]. Molecular characterization is therefore crucial for understanding, predicting and controlling PEG surface characteristics. IR spectroscopy is a specialized analytical method for the detection of conformational variations based on the advantage that bands related to repeating unit sequences in crystalline, amorphous and intermediate phases are observed independently in the IR spectra [9]. The objective of this study is to investigate the adsorption and organization of crystalline PEG polymer in thin films. In that way, polarization modulation infrared reflection–absorption spectrometry (PM-IRRAS) is used to access the PEG chain conformational states when physisorbed as thin films on a substrate. The measure of surface PM-IRRAS spectra is possible due to the differential reflectivity of p- and s-polarized light [10,11]. The magnification of the electric field at the PEG/substrate interface allows inferring PEG adsorption, structuration and conformational changes induced by PEG/substrate interactions. The gold-coated glass substrate was chosen for its high reflectance and low roughness, as well as its chemical and inertness properties to provide insight into the effects of confinement on adsorption and PEG polymer chain structure. The advantage of gold is also the possibility to modify its surface chemistry by thiol grafting. Therefore, the influence of the chemistry of the substrate (hydrophilic vs. hydrophobic) on the adsorption and structuration of PEG thin films will be studied. In addition to spectroscopic analysis, the surface topology of the PEG thin films and their ability to crystallize at solid interfaces were examined by atomic force microscopy (AFM).

## 2. Materials and Methods

### 2.1. Materials

Polyethylene glycol with  $M_n = 2050 \text{ g.mol}^{-1}$  (Sigma Aldrich, St. Louis, MO, USA) and conditioned as flakes was used as received for the bulk characterization by infrared attenuated total reflection (ATR) spectroscopy. The formula of this polymer is given in Figure 1. Several studies characterized the high crystallinity of PEG varying from 85.7% to 87.2% for  $M_n = 1000 \text{ g.mol}^{-1}$  and  $M_n = 3400 \text{ g.mol}^{-1}$ , respectively [12]. PEG with  $M_n = 2000 \text{ g.mol}^{-1}$  has been studied by Li et al. [13], revealing a degree of crystallinity equal to 94%.

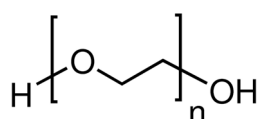


**Figure 1.** Formula of polyethylene glycol (PEG).

For the PM-IRRAS experiments, PEG was dissolved in THF ( $5 \text{ g.L}^{-1}$ ) and spin-coated (1000 rpm for 30 s) on different substrates. The thin films were dried in ambient air. The thicknesses of the films were around 20 nm. In order to better understand the effect of adsorption on the chain organization at the solid surface, PEG was spin-coated from solutions on gold-coated glass substrates. This substrate offers two main advantages for the study: a highly reflective surface for the PM-IRRAS spectroscopic analysis and also a weak surface roughness for atomic force microscopy (AFM) analysis. Gold-coated substrates were prepared using glass slides, firstly cleaned by ultrasound for 5 min in a distilled water bath, then rinsed with acetone and ethanol. They were finally dried in an oven for 10 min at  $80 \text{ }^\circ\text{C}$ . In order to ensure that the gold layer remains on the glass slide during chemical grafting, it is necessary to use a coupling agent between the glass slide and the gold layer. The surface was activated (surface enrichment with silanol groups) by immersion of the cleaned glass slides in a piranha solution ( $70\% \text{ H}_2\text{SO}_4 + 30\% \text{ H}_2\text{O}_2$ ) at  $50 \text{ }^\circ\text{C}$  for 15 min. A solution of 3-mercaptoptriethoxysilane (ABCRC) dissolved in toluene was used as a coupling agent between the glass slide and the gold layer. Quickly after rinsing with toluene a

50 nm thin layer of gold was deposited using a Cressington Serie 108 metallizer (Cressington Scientific Instruments, Watford, UK) under argon.

The influence of the substrate chemistry was studied with the development of hydrophobic and hydrophilic substrates. The thiol molecules used for the gold-coated substrate functionalization are the following: hexadecanethiol (Sigma Aldrich) for the hydrophobic substrate (end-group  $\text{CH}_3$ ) and cysteamine (Sigma Aldrich) for the hydrophilic substrate (end-group  $\text{NH}_2$ ). Gold-coated glass substrates were immersed at room temperature in graft solutions of thiols at a concentration of  $3 \text{ mmol}\cdot\text{L}^{-1}$  dissolved in toluene for hexadecanethiol and a water/ethanol mixture for cysteamine. The immersion time in the grafting solution was fixed at 30 min for the hydrophilic substrate and 18 h for the hydrophobic substrate. After the adsorption procedure, the substrates were washed with toluene or ethanol to remove ungrafted thiol molecules and then dried. The chemically grafted gold substrates are schematically represented in Figure 2.

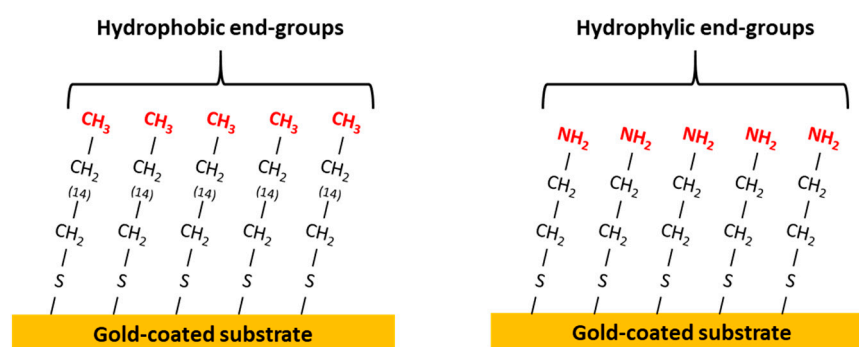


**Figure 2.** Hydrophobic ( $\text{Au-CH}_3$ ) and hydrophilic ( $\text{Au-NH}_2$ ) substrates obtained by chemical grafting of gold-coated glass substrates.

The complete covering of the grafted surface with thiols and also the wettability of the different substrates used in this study have been characterized by water contact angle measurements. Water droplets have a contact angle of  $60^\circ$  on the Au substrate, indicating partial wetting. The contact angle is reduced to  $21^\circ$  on the  $\text{Au-NH}_2$  substrate, which can be considered a hydrophilic substrate. Water droplets show a contact angle of  $109^\circ$  on the  $\text{Au-CH}_3$  substrate, which can be considered a hydrophobic substrate. These values are in agreement with the literature [14].

## 2.2. Methods

### 2.2.1. Infrared Spectroscopy

- Attenuated Total Reflection (ATR)

Bulk PEG homopolymer was analyzed by single-reflection attenuated total reflection (ATR) infrared spectroscopy. Measurements were performed directly on PEG pellets with a Bruker Vertex 70 FTIR spectrometer (Bruker France SAS, Wissembourg, France) coupled to a Bruker Platinum ATR module mounted on a universal QuickLock device in the sample compartment. The ATR module is equipped with a diamond single-reflection crystal. The FTIR spectrum of PEG homopolymer was acquired from  $4000$  to  $400 \text{ cm}^{-1}$ . The number of scans was fixed at 50 with a resolution of  $4 \text{ cm}^{-1}$ . The reproducibility of the results was systematically checked. Spectral data were processed using the Bruker software system Opus 7.5.

- Polarization-Modulation Infrared Reflection-Absorption Spectroscopy (PM-IRRAS)

Since the amount of polymer deposited on the metal substrate is very small, it is very difficult to characterize the interface using conventional FTIR spectroscopy. PEG thin films on Au,  $\text{Au-CH}_3$  and  $\text{Au-NH}_2$  substrates were characterized by PM-IRRAS. This method detects an infrared beam that is polarized, doubly modulated, and then reflected from a surface, as shown in Figure 3. The difference in reflectivity of the two polarization

components (s and p) is characteristic of the adsorption of the surface layers [15,16]. Thanks to the special selection rules caused by the polarization modulation and after mathematical demodulation of the signals, the measurement sensitivity is increased, and the signal noise is reduced [17], allowing molecular layer analysis of thicknesses in the nm range.

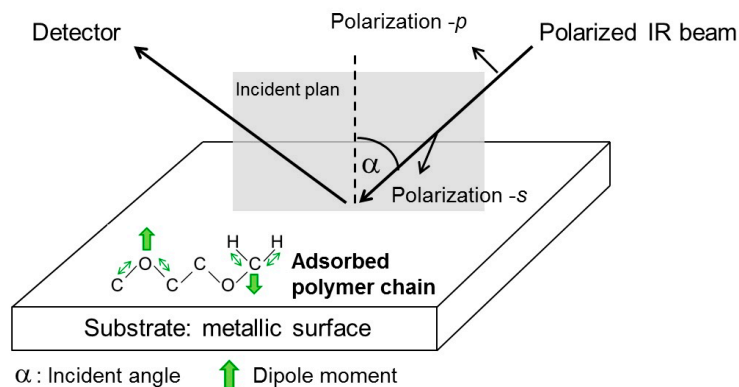


**Figure 3.** Scheme of the PM-IRRAS principle.

In addition to the high sensitivity and noise reduction, the selection rules at the reflection point of the IR waves imply a relation between the change in dipole moment direction for a given mode of vibration of a bond and the intensity of the corresponding PM-IRRAS absorption band. This technique is well known for providing access to the orientation of polymer chains adsorbed on a reflective substrate as thin films [18,19]. Indeed, when the dipole moment of a bond is oriented perpendicularly to the surface, the corresponding PM-IRRAS band is intensified. On the contrary, when the dipole moment is oriented parallel to the surface, the corresponding PM-IRRAS band is off. PM-IRRAS experiments were performed using a Bruker Vertex 70 FTIR spectrometer (Bruker France SAS, Wissembourg, France) equipped with a Bruker PMA 50 external optical rack for reflectance–absorption analysis. The module includes a photoelastic modulator (Hinds Instruments PM 100 (Hinds Instruments, Hillsboro, OR, USA)) with a 50 kHz ZnSe optical head, an MCT detector, and an SRS 830 lock-in amplifier (Stanford Research Systems, Sunnyvale, CA, USA) for synchronous demodulation of the signal. PM-IRRAS spectra of PEG thin films were recorded in the range of 4000–400  $\text{cm}^{-1}$ . The conditions for acquiring spectra were fixed at: 1000 scans and a resolution of 4  $\text{cm}^{-1}$ . All substrates were placed in a vertical configuration with an IR beam incidence angle of 80°, close to the grazing incidence angle. The reproducibility of the results was systematically checked. Spectral data were analyzed using the Bruker Opus 7.5 software package.

- Infrared Spectra Treatments

Several treatments were applied to both ATR and PM-IRRAS spectra in order to obtain the optimal spectral quality for the interpretation of the results. Diffusion, chromatic distortion and light diffraction are phenomena occurring when the infrared beam goes through the polymer sample in the bulk state or as thin films. A part of the light is thus deviated and does not reach the detector anymore, leading to an inclination of the baseline of the infrared spectra that is more or less important. A baseline correction was systematically applied to spectra. Unambiguous identification of the precise wavenumbers of characteristic IR vibration bands on each spectrum needs application of a second derivative mathematical treatment to the initial spectrum. The OPUS 7.5 software was used in that way. This function improves the resolution of the IR vibration bands, leading to more precise information in terms of band contribution and position.

### 2.2.2. Atomic Force Microscopy (AFM)

AFM images of PEG thin films adsorbed on Au, Au-CH<sub>3</sub> and Au-NH<sub>2</sub> were obtained using a Bruker Dimension Edge AFM coupled to the Nanodrive 8.1 controller. AFM tips

were supplied by Veeco Instruments, Plainview, NY, USA. All experiments were performed in contact mode. Tips are made of silicon nitride ( $\text{Si}_3\text{N}_4$ ) with a gold reflective coating on the back side. The cantilever geometry is triangular, the spring constant is 0.35 N/m, allowing high sensitivity, and the tip radius is around 2 nm, allowing high vertical and lateral resolution. Scan sizes were fixed at  $90\ \mu\text{m} \times 90\ \mu\text{m}$  and  $10\ \mu\text{m} \times 10\ \mu\text{m}$ , and the scan frequency (lines/s) was fixed at 1 Hz. The AFM raw signal was recorded in deflection mode. The reproducibility of the results was systematically checked.

### 3. Results

#### 3.1. PEG Bulk Characterization Investigated by ATR

In order to better understand how semi-crystalline PEG is organized when adsorbed on a substrate, the IR spectral fingerprint of bulk PEG is firstly investigated. The FTIR attenuated total reflection (ATR) was performed on PEG pellets to assign the IR absorption bands observed in the spectrum to the corresponding bonds, functional groups and vibration modes. The coordinates of normal vibrations used for peak assignments are the following:

- $\nu_a$ : Antisymmetric stretching mode;
- $\nu_s$ : Symmetric stretching mode;
- $\delta$ : Scissoring bending mode (in plane);
- $\gamma_r$ : Rocking bending mode (in plane);
- $\gamma_w$ : Wagging bending mode (out of plane);
- $\gamma_t$ : Twisting (or torsion) bending mode (out of plane).

The mid-IR ATR spectrum of PEG is given in Figure 4. Figure 5 represents a focus on the  $3100\text{--}2600\ \text{cm}^{-1}$ ,  $1500\text{--}1200\ \text{cm}^{-1}$  and  $1200\text{--}400\ \text{cm}^{-1}$  spectral regions. The positions and assignments of the IR absorption bands of the PEG spectrum shown in Figures 4 and 5 will refer to group theory spectral analysis available in the literature studies of PEG [20–23].

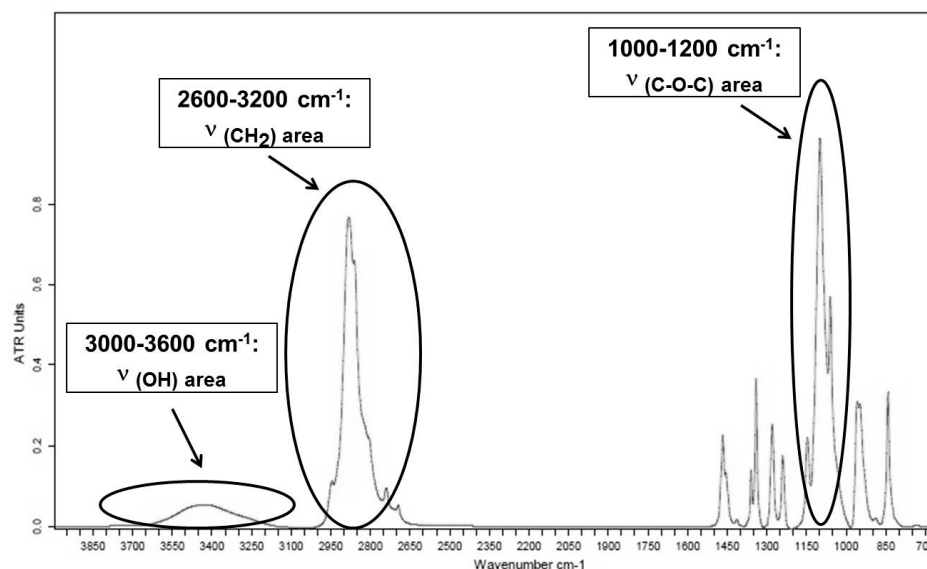


**Figure 4.** Infrared spectrum (ATR) of PEG in the  $4000$  to  $700\ \text{cm}^{-1}$  region.

Detailed information about the infrared absorption bands observed in PEG in the spectral regions from  $2600$  to  $3100\ \text{cm}^{-1}$ , from  $1200$  to  $1500\ \text{cm}^{-1}$  and from  $800$  to  $1200\ \text{cm}^{-1}$  is reported in Figure 5a, Figure 5b and Figure 5c, respectively. The IR band assignments of PEG are presented in Table 1.

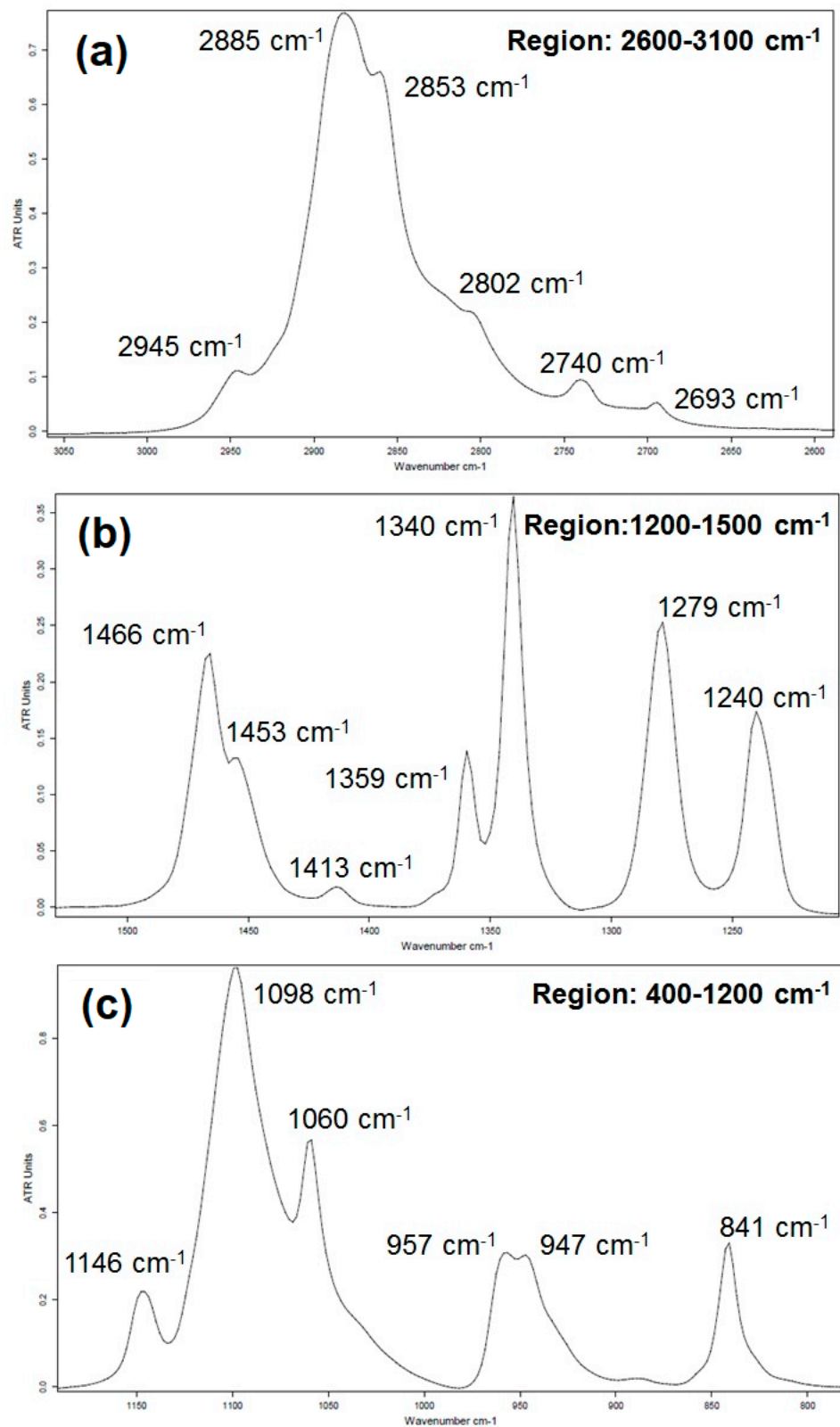


**Figure 5.** Infrared spectrum (ATR) of PEG in the region (a) 3100 to 2600  $\text{cm}^{-1}$ , (b) 1500 to 1200  $\text{cm}^{-1}$  and (c) 1200 to 800  $\text{cm}^{-1}$ .

**Table 1.** IR band assignments for bulk PEG infrared spectrum (ATR).

Wavenumbers (cm <sup>-1</sup> )	Assignment	Phase	Orientation	Intensity
3408	$\nu(\text{OH})$	-	-	Weak-Broad
2945	$\nu_a(\text{CH}_2)$ out of plane + $\nu_a(\text{CH}_3)$	A; C	-	Weak
2885	$\nu_a(\text{CH}_2)$	-	//	Strong
2853	$\nu_s(\text{CH}_2)$	A	$\perp$	Strong
2802	$\nu_a(\text{CH}_2)$	-	//	Weak
2740	$\delta_a(\text{CH}_2)$ + $\gamma_t(\text{CH}_2)_a$ + $\gamma_t(\text{CH}_2)_s$	-	//	Weak
2693	$\delta_a(\text{CH}_2)$ + $\gamma_t(\text{CH}_2)_a$	-	$\perp$	Very weak
1466	$\delta_s(\text{CH}_2)$	C	$\perp$	Medium
1453	$\delta_a(\text{CH}_2)$ + $\delta_s(\text{CH}_2)$	A; C	$\perp$	Medium
1413	$\gamma_w(\text{CH}_2)_a$	-	$\perp$	Weak
1359	$\gamma_w(\text{CH}_2)_s$	C	$\perp$	Medium
1340	$\gamma_w(\text{CH}_2)_a$	C	//	Strong
1279	$\gamma_t(\text{CH}_2)_a$ + $\gamma_t(\text{CH}_2)_s$	A; C	$\perp$	Medium
1240	$\gamma_t(\text{CH}_2)_a$	C	$\perp$	Medium
1146	$\nu(\text{C-C})$ + $\nu_a(\text{C-O-C})$	C	//	Strong
1098	$\nu_a(\text{C-O-C})$	C	//	Very strong
1060	$\nu_s(\text{CH}_2)$ + $\nu_a(\text{C-O-C})$	C	//	Strong
957	$\gamma_r(\text{CH}_2)$	C	$\perp$	Medium
947	$\gamma_r(\text{CH}_2)$ + $\nu_a(\text{C-O-C})$	A; C	//	Medium
841	$\gamma_r(\text{CH}_2)_a$	C	//	Strong

The PEG's infrared absorption band assignments are compiled in Table 1. An indication of whether they belong to the crystalline (C) or amorphous (A) phases is reported. Table 1 also gathers each band's dipole moment orientation with respect to the main chain axis. An oscillating dipole moment parallel and perpendicular to the C-C chain axis is represented by the orientations // and  $\perp$ , respectively. Further analysis of the molecular orientation effects caused by confinement when adsorbed as thin films on Au substrate and chemically modified Au-CH<sub>3</sub> and Au-NH<sub>2</sub> substrates will benefit from this information.

The analysis of the crystalline and/or amorphous contributions of the IR vibration bands provides qualitative information about PEG crystallinity in the bulk state. According to reference works [20,21], one can consider the following vibration modes as pure modes related to the crystalline phase, namely:

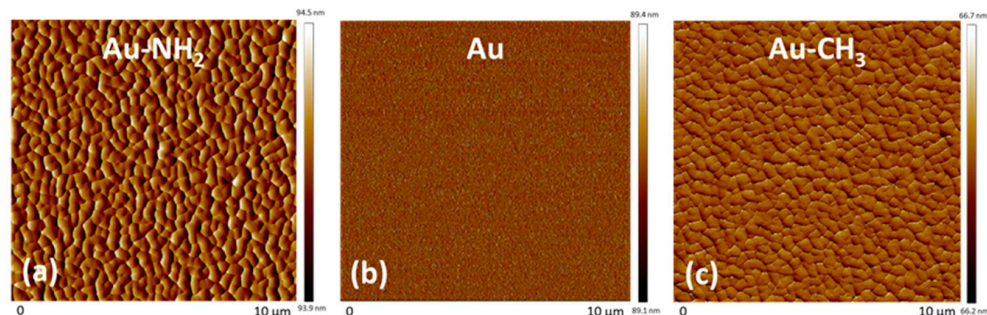
- the  $\delta_s(\text{CH}_2)$  bending mode at 1466 cm<sup>-1</sup> and the  $\gamma_w(\text{CH}_2)$  wagging mode doublet at 1340 cm<sup>-1</sup> and 1359 cm<sup>-1</sup>;
- the triplet of the  $\nu_a(\text{C-O-C})$  antisymmetric stretching mode at 1060 cm<sup>-1</sup>, 1098 cm<sup>-1</sup> and 1146 cm<sup>-1</sup>;
- the  $\gamma_r(\text{CH}_2)_a$  antisymmetric rocking mode at 841 cm<sup>-1</sup> and the  $\gamma_r(\text{CH}_2)$  rocking modes of CH<sub>2</sub> at 957 cm<sup>-1</sup> and 947 cm<sup>-1</sup>.

All these vibration modes have medium or strong intensities on the IR spectrum allowing them to be used for further determination of conformational analysis and crystallinity changes due to confinement in thin films.

### 3.2. Adsorption of PEG Thin Films on Model Substrates

#### 3.2.1. Surface Topology of Model Substrates

The surface topology of the Au, Au-NH<sub>2</sub> and Au-CH<sub>3</sub> substrates was investigated by AFM in contact mode (Figure 6).



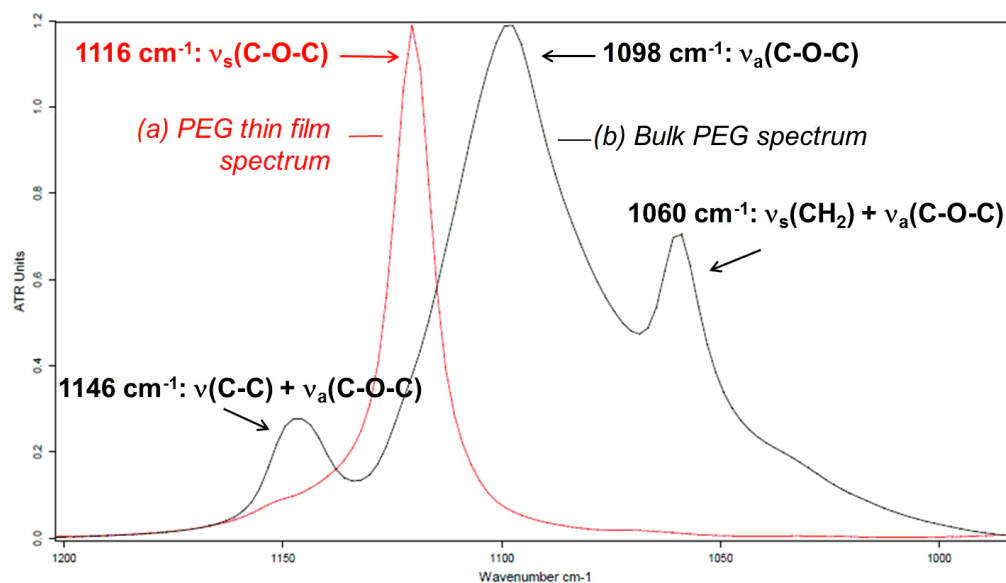
**Figure 6.** AFM pictures of the deflection signal in contact mode (10 μm × 10 μm) for (a) Au-NH<sub>2</sub> substrate, (b) Au substrate and (c) Au-CH<sub>3</sub> substrate.

Figure 6b shows that gold deposition on the glass slide allows obtaining a homogeneous gold-coated substrate from the topographic point of view with a very low roughness, i.e., Ra = 0.2 nm. Figure 6a,c show that hexadecanethiol and cysteamine molecules used for the gold-coated substrate functionalization achieve efficient and complete covering of the Au substrate. Moreover, they self-organize into nanodomains of some hundreds of nm. The substrate surface roughnesses are very low, i.e., Ra = 0.7 nm and Ra = 0.6 nm, respectively, for Au-NH<sub>2</sub> and Au-CH<sub>3</sub> substrates. These low roughness values will first allow high reflection of the IR wave in PM-IRRAS mode and second, are much lower than the radius of gyration of a single PEG chain, rendering feasible the observation of PEG chain morphology by using AFM.

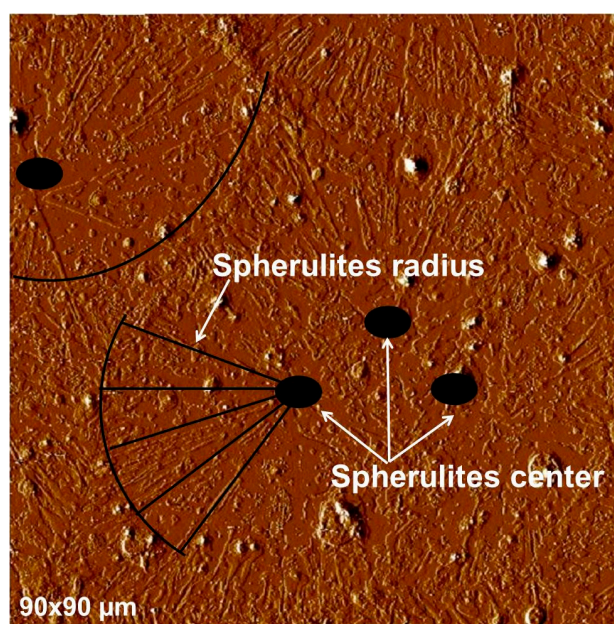
#### 3.2.2. Adsorption on Gold Substrate (Au): Effect on PEG Chain Organization

Figure 7 compares the spectrum of bulk PEG obtained by ATR and the spectrum of PEG thin film adsorbed on the gold-coated substrate (referred to as Au) obtained by PM-IRRAS, for the IR spectral region ranging from 1000 cm<sup>-1</sup> to 1200 cm<sup>-1</sup> and from 2600 cm<sup>-1</sup> to 3100 cm<sup>-1</sup>, respectively. The comparison of these spectra is relevant to the effect of the adsorption on the PEG chain orientation. The effect is particularly significant in the region of the ν(C-O-C) stretching vibration modes between 1000 cm<sup>-1</sup> and 1200 cm<sup>-1</sup> presented in Figure 7.

The extinction of the band at 1098 cm<sup>-1</sup> corresponds to the extinction of the ν<sub>as</sub>(C-O-C) band. The bands at 1060 cm<sup>-1</sup> and 1146 cm<sup>-1</sup> are combination bands and their extinction also corresponds to the ν<sub>as</sub>(C-O-C), as their frequencies are located between 1000 cm<sup>-1</sup> and 1200 cm<sup>-1</sup>, in the region of the C-O-C absorption. The asymmetric stretching mode of C-O-C has a dipole moment parallel to the chain axis and thus parallel to the Au substrate, as this mode is off on the PM-IRRAS spectrum. The parallel orientation of the C-O-C bonds with the Au substrate can be explained by the affinity (partial wetting) of the hydrophilic PEG chains, and especially the oxygen atoms present in C-O-C, with the Au substrate. A single peak emerges at 1116 cm<sup>-1</sup> on the spectrum corresponding to the symmetric stretching mode ν<sub>s</sub>(C-O-C). The appearance of the ν<sub>s</sub>(C-O-C) symmetric stretching mode with a dipole moment perpendicular to the chain axis supports the hypothesis of the orientation of chains parallel to the Au surface. The extinction of the crystalline peaks at 1060 cm<sup>-1</sup>, 1098 cm<sup>-1</sup> and 1146 cm<sup>-1</sup> with the appearance of a single peak emerging at 1116 cm<sup>-1</sup> is interpreted as an amorphization of PEG [21]. To confirm this amorphization, the surface topography and morphology of the PEG thin film adsorbed on the Au substrate were investigated by atomic force microscopy (AFM) in contact mode (Figure 8).



**Figure 7.** Comparison of the infrared spectra of PEG thin film adsorbed on Au (PM-IRRAS) (red line) and bulk PEG (ATR) (black line) in the  $\nu(\text{C-O-C})$  region from  $1000$  to  $1200\text{ cm}^{-1}$ .



**Figure 8.** AFM picture of the deflection signal in contact mode for PEG thin film spin-coated on Au substrate ( $90\text{ }\mu\text{m} \times 90\text{ }\mu\text{m}$ ).

As seen in Figure 8, a homogeneous layer of PEG covers the gold-coated glass surface indicating PEG chains have an affinity with the Au surface. PEG deposited on Au is mainly arranged radially around a center. The radial orientations of the polymer around a center are attributed to spherulites, crystalline structures characteristic of PEG [24]. In a previous study [25], we have extensively investigated the crystalline behavior of PEG chains using thermal analysis (DSC) and cross-polarized optical microscopy. The PEG melting temperature was found to be equal to  $52\text{ }^{\circ}\text{C}$ , and the degree of crystallinity was found to be equal to 95%. Primary and secondary crystallizations were observed by cross-polarized optical microscopy, and spherulite sizes (radius up to  $100\text{ }\mu\text{m}$ ) and growth rates (up to  $20\text{ }\mu\text{m}\cdot\text{s}^{-1}$ ) were recorded as a function of crystallization temperature. This study [25] clearly underlines the crystalline structure in the PEG structure. However, when PEG is spin-coated on gold, the spherulites are only partially formed and not well visible com-

pared to conventional spherulites observed for bulk highly crystalline PEG [25–29]. This observation supports the hypothesis of the PEG amorphization due to polymer adsorption on the Au substrate, as indicated by the extinction of IR crystalline bands on the PM-IRRAS spectrum (Figure 7), and reveals that the PEG/Au interactions are predominant compared to the interchain PEG/PEG interactions.

### 3.2.3. Influence of the Substrate Chemistry on PEG Chain Organization

Thin films of PEG are deposited on a hydrophilic substrate (Au-NH<sub>2</sub>) and on a hydrophobic substrate (Au-CH<sub>3</sub>). These substrates were developed by chemical grafting of thiols on gold metallic substrates and have different wetting properties, as described in the “Materials” section. The regions of CH<sub>2</sub> bond stretching modes between 2700 cm<sup>-1</sup> and 3000 cm<sup>-1</sup>, and C-O-C bond stretching modes ranging from 1000 cm<sup>-1</sup> to 1200 cm<sup>-1</sup> being the most sensitive and the most intense, interpretation of the spectra will be carried out for these two spectral zones. Figure 9 compares the PM-IRRAS spectra of PEG thin films deposited on ungrafted Au substrate, on the Au-NH<sub>2</sub> hydrophilic substrate, and on the Au-CH<sub>3</sub> hydrophobic substrate, in the  $\nu(\text{CH}_2)$  stretching vibration mode region.

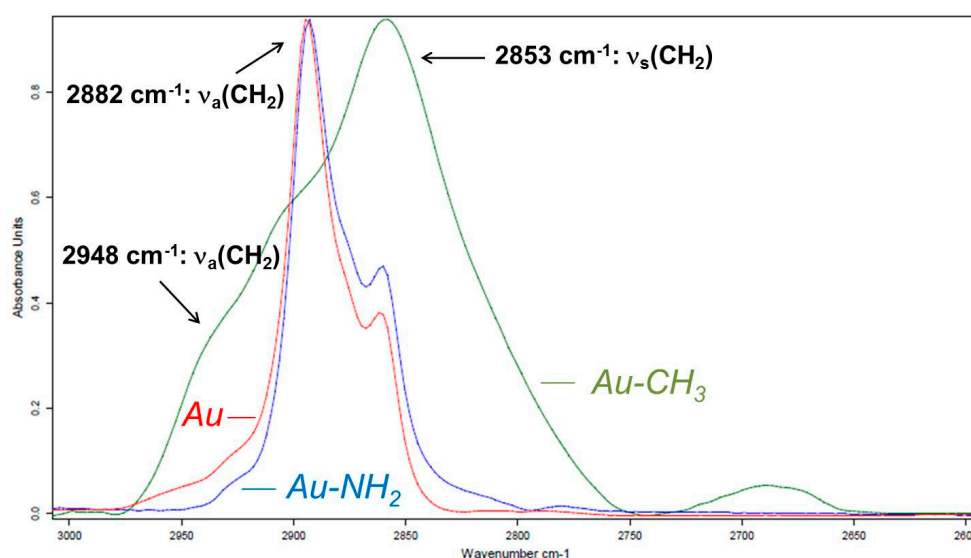


**Figure 9.** Infrared spectrum of PEG thin film adsorbed on Au substrate (red line), Au-CH<sub>3</sub> hydrophobic substrate (green line), and Au-NH<sub>2</sub> hydrophilic substrate (blue line), in the 2600 to 3000 cm<sup>-1</sup>  $\nu(\text{CH}_2)$  absorption zone.

When the substrate is hydrophobic (Au-CH<sub>3</sub>), a broad absorption band with several contributions appears. Indeed, the absorption band at 2853 cm<sup>-1</sup> corresponding to the symmetric  $\nu_s(\text{CH}_2)$  stretching mode is strongly intensified. The same is true for the asymmetrical (out-of-plane) stretching mode at 2948 cm<sup>-1</sup>, but because this band is not pure ( $\nu_a(\text{CH}_2)$  out of plane +  $\nu_a(\text{CH}_3)$ ), it will not be considered for quantitative analysis. The asymmetric  $\nu_a(\text{CH}_2)$  absorption band at 2882 cm<sup>-1</sup> is reduced in intensity. The increase in the width at the half-height of the absorption bands on the hydrophobic Au-CH<sub>3</sub> substrate as well as the enhancement of the  $\nu_s(\text{CH}_2)$  mode at 2853 cm<sup>-1</sup> correspond to an amorphization of the PEG.

The hydrophilic substrate (Au-NH<sub>2</sub>) thus seems to be a more favorable surface for the crystallization of PEG than the hydrophobic substrate. However, not all spectral changes of the PEG in a thin film adsorbed on the Au-CH<sub>3</sub> substrate correspond to the characteristics of amorphization in this region. In addition, the qualitative interpretation of the PM-IRRAS spectra does not allow conclusions to be drawn on the PEG chain orientation relative to the hydrophobic substrate. Quantitative determination of the average angles of inclination

of the PEG chains relative to the substrate can then turn out to be essential to access the organization of the PEG chains at these different interfaces.

#### 4. Discussion

##### 4.1. Quantitative Spectrum Analysis

The quantitative approach consists of deducing, from the PM-IRRAS infrared spectra of adsorbed PEG thin films, the angle of inclination of the macromolecular backbone axis relative to the surface of the substrate. This is accomplished by computing the value of the angle  $\theta$ , which is defined by the following equation [30] and represents the angle between the dipole moment and the normal to the surface plane.

$$\cos^2(\theta) = \frac{I_{\text{anisotropic}}}{3 \cdot I_{\text{isotropic}}} \quad (1)$$

With  $I_{\text{anisotropic}}$  the intensity measured experimentally for a thin polymer film adsorbed on a substrate (PM-IRRAS) and  $I_{\text{isotropic}}$  the measured intensity for the same polymer in the bulk state (ATR). In the case of a vibration mode whose transition moment is perpendicular to the chain axis, like the symmetrical elongation mode, the angle  $\varphi$  corresponds to the angle between the dipole moment and the chain axis (see Figure 10), and the angle  $\alpha$  corresponds to the angle between the chain backbone axis and the plane of the substrate. Indeed,  $\alpha$  is related to  $\varphi$  according to:

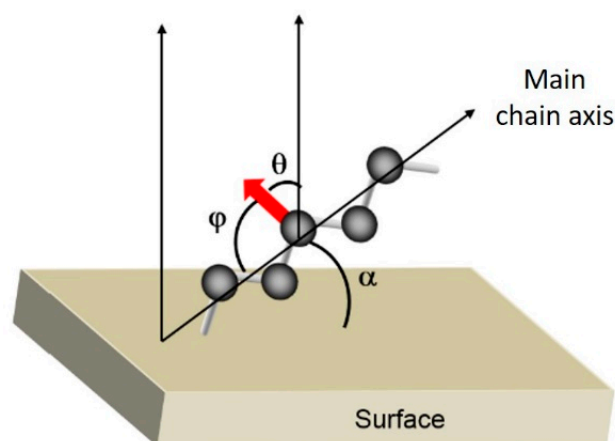


**Figure 10.** Scheme of orientation angles for a vibration mode with an oscillating dipole (red arrow)  $\perp$  to the main chain axis. Reproduced from [19], with permission from Elsevier, 2024.

$\alpha = \theta$  for a vibration mode with an oscillating dipole perpendicular to the chain axis;  
 $\alpha = \pi/2 - \theta$  for a vibration mode with an oscillating dipole parallel to the chain axis.

The application of PM-IRRAS selection rules and quantitative determination of orientation angles imposes that IR bands satisfy several criteria, namely, to be intense and pure. The orientation of adsorbed polymer chains relative to the substrate, can thus be determined quantitatively by FTIR in PM-IRRAS mode according to Equation (1).

In the case of PEG, a pure and strong absorption band whose vibration mode corresponds to a dipole moment oriented  $\perp$  to the chain axis is the  $\nu_s(\text{CH}_2)$  absorption band at  $2853 \text{ cm}^{-1}$ . To obtain the inclination of the PEG chains relative to the substrate it is necessary to first carry out a spectral decomposition of the region between  $2600 \text{ cm}^{-1}$  and  $3000 \text{ cm}^{-1}$ . The positions of the absorption bands are determined by the second derivative treatment of each ATR (bulk) and PM-IRRAS (thin film) PEG spectrum. A comparison of PM-IRRAS and ATR infrared spectra of PEG in the  $\nu(\text{CH}_2)$  absorption region from  $2600$  to  $3100 \text{ cm}^{-1}$  is represented in Figure 11.

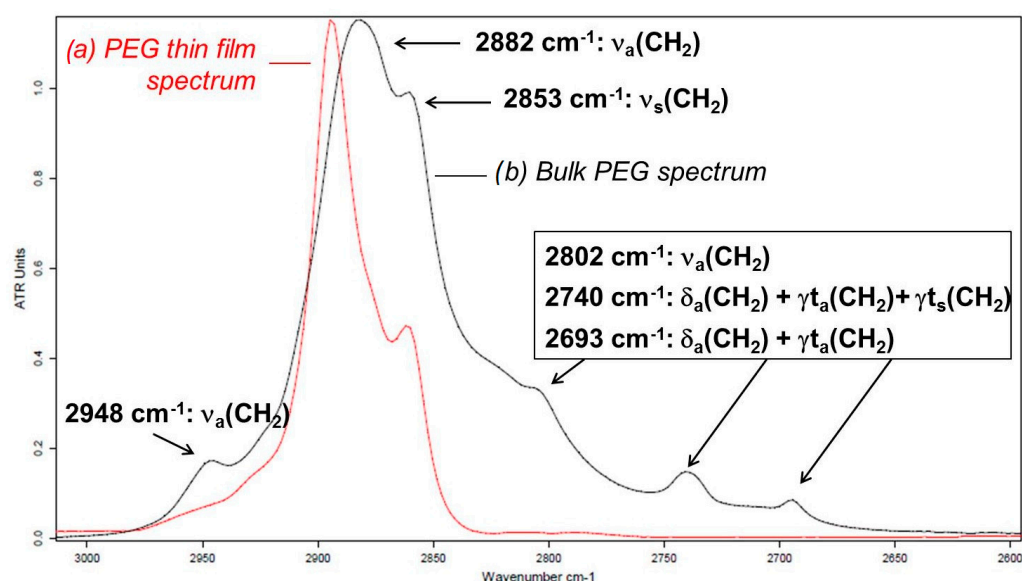


**Figure 11.** Comparison of the (a) thin film PM-IRRAS and (b) bulk ATR infrared spectra of PEG in the  $3100$  to  $2600$   $\text{cm}^{-1}$   $\nu(\text{CH}_2)$  absorption region.

To perform quantitative analysis, a spectral decomposition where multiple IR bands overlap is needed. To unambiguously identify the precise wavenumbers of characteristic IR vibration bands that overlap, a second derivative mathematical treatment of the initial spectrum was applied. This function improves the resolution of the IR vibration bands, leading to more precise information in terms of band contribution and position. Figure 12 reports an example for the ATR spectrum of PEG in the region of  $\text{CH}_2$  stretching vibration modes. The “FIT” spectrum corresponds to the ATR spectrum obtained by the sum of individual contributed bands (red line + blue lines), resulting from spectral decomposition.

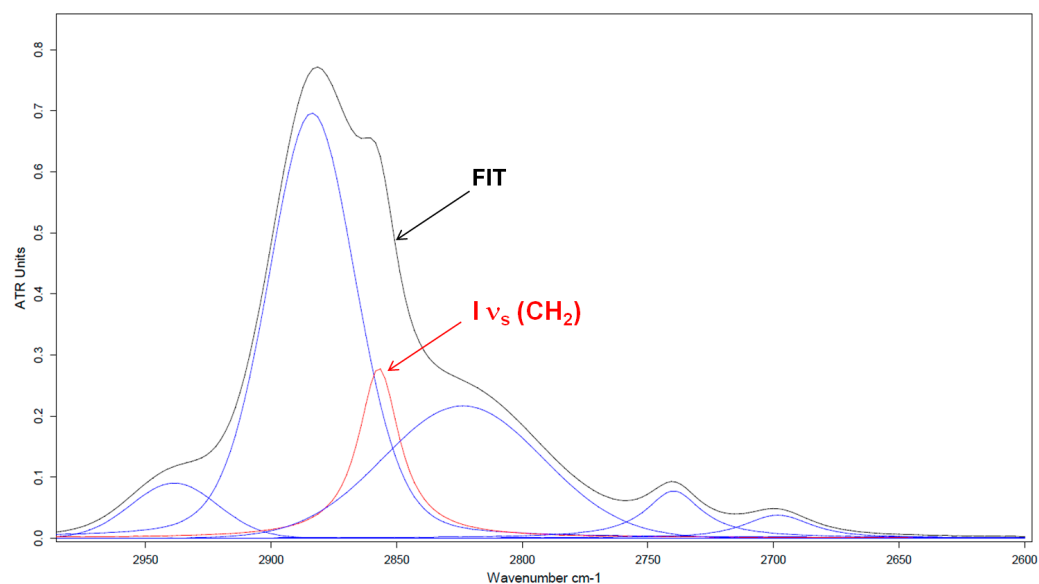


**Figure 12.** Spectral decomposition of bulk PEG ATR spectrum in the  $2600$  to  $3000$   $\text{cm}^{-1}$  region. FIT spectrum (black line) corresponds to the sum of individual contributed bands (red line + blue lines).

After spectral decomposition, the area (integrated intensity,  $I$ ) of the band at  $2853$   $\text{cm}^{-1}$  of the ATR spectrum is compared to the area of the same band of the PM-IRRAS spectrum representative of PEG adsorbed in thin film on different substrates. The area of the absorption band of the different PM-IRRAS spectra requires setting identical

values of the position (wavenumber) and the half-height width for the ATR spectrum and the PM-IRRAS spectrum. From these areas and Equation (1), the angle  $\alpha$  between the chain axis and the substrate surface is deduced. The values of the areas of the absorption band  $\nu_s(\text{CH}_2)$  at  $2853\text{ cm}^{-1}$  and orientation angles of the macromolecular chain axis with respect to different substrates are given in Table 2 below.

**Table 2.** Band half-widths, band areas, and PEG chain inclination angle  $\alpha$  values calculated from the  $\nu_s(\text{CH}_2)$  band at  $2853\text{ cm}^{-1}$  on substrates of various surface chemistries.

PEG	IR Mode	Width ( $\text{cm}^{-1}$ )	I $\nu_s(\text{CH}_2)$	$\alpha$ ( $^\circ$ )
Bulk	ATR	28	0.386	-
Film on Au		28	0.093	16
Film on Au-NH <sub>2</sub>	PM-IRRAS	28	0.034	10
Film on Au-CH <sub>3</sub>		28	0.900	62

From the values of the angle  $\alpha$ , we observe that the inclination of the PEG chains relative to the surface of the substrate is relatively close for the gold substrate (Au) and for the hydrophilic substrate (Au-NH<sub>2</sub>). This trend confirms the hypotheses that the PEG chains are oriented rather // to the surface for both substrates whose contact angles are less than  $90^\circ$  with water. Conversely, the PEG chains tilt significantly on the hydrophobic Au-CH<sub>3</sub> substrate, reaching an average angle of  $62^\circ$  relative to the plane of the substrate. The fact that PEG chains have a rather hydrophilic character and have little affinity for the hydrophobic surface (hydrophilic/hydrophobic repulsion) could be an explanation. PEG/hydrophobic substrate interactions being disadvantaged, the spectral response of stretching vibration modes of C-O-C bonds between  $1000\text{ cm}^{-1}$  and  $1200\text{ cm}^{-1}$ , which is a region sensitive to PEG crystalline phase, could contribute to understanding the organization of PEG chains. In the C-O-C stretching vibration modes spectral domain, Figure 13 compares the PM-IRRAS spectra of the PEG thin film deposited on the gold substrate (Au) and on both hydrophilic (Au-NH<sub>2</sub>) and hydrophobic (Au-CH<sub>3</sub>) substrates.

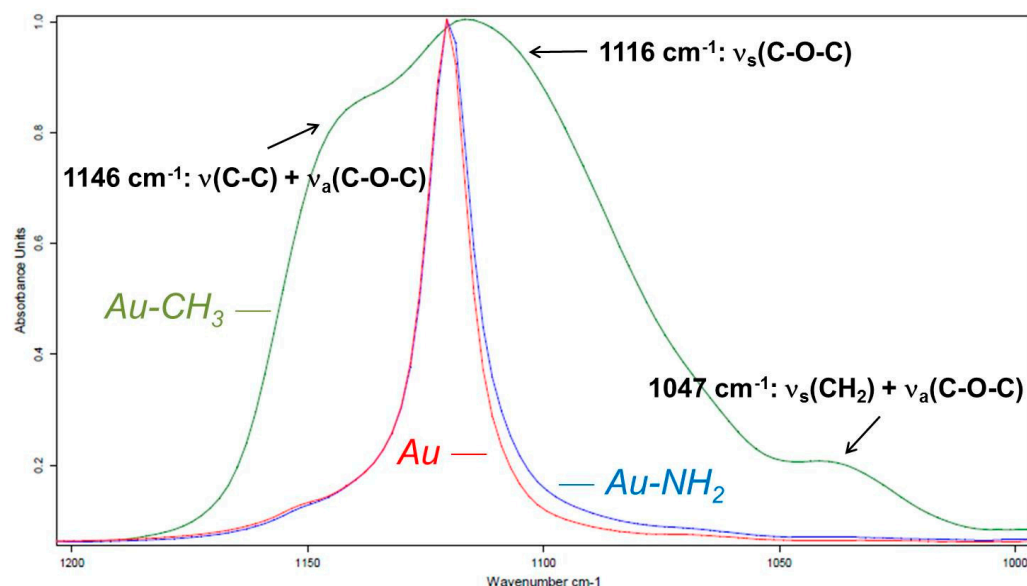


**Figure 13.** Infrared spectrum of PEG thin film adsorbed on a gold-coated substrate (Au) (red line), hydrophobic substrate (Au-CH<sub>3</sub>) (green line), and hydrophilic substrate (Au-NH<sub>2</sub>) (blue line) in the  $\nu(\text{C-O-C})$  spectral domain from  $1000$  to  $1200\text{ cm}^{-1}$ .

The same trend is observed in this region of the infrared spectrum for PEG adsorbed on a hydrophobic substrate: several wide absorption bands replace the narrow absorption

bands of more hydrophilic substrates. Indeed, the  $1146\text{ cm}^{-1}$  combination band is highly enhanced and an amorphous phase band at  $1047\text{ cm}^{-1}$  appears. These two observations are characteristic of the amorphization of PEG, as described previously. This amorphization indicates that the inclined PEG chains relative to the hydrophobic substrate do not organize themselves into lamellae due to their non-stable conformation on this type of substrate. The  $\nu_s(\text{C-O-C})$  band at  $1116\text{ cm}^{-1}$  corresponds to symmetrical stretching modes with a vibrating dipole  $\perp$  to the main chain PEG axis. The area of this band calculated from the ATR spectrum can thus be compared to the area of the same band calculated from PM-IRRAS spectra of PEG adsorbed on different substrates. The values of the integrated intensities of the  $\nu_s(\text{C-O-C})$  band at  $1116\text{ cm}^{-1}$  and the orientation angles of the PEG chains with respect to different substrates are given in Table 3.

**Table 3.** Band half-widths, band areas and PEG chain inclination angle  $\alpha$  values calculated from the symmetrical  $\nu_s(\text{C-O-C})$  band at  $1116\text{ cm}^{-1}$  on substrates of various surface chemistries.

PEG	IR Mode	Width ( $\text{cm}^{-1}$ )	I $\nu_s(\text{CH}_2)$	$\alpha$ ( $^\circ$ )
Bulk	ATR	29.5	0.946	-
Film on Au		29.5	0.676	29
Film on Au-NH <sub>2</sub>	PM-IRRAS	29.5	0.523	25
Film on Au-CH <sub>3</sub>		29.5	1.732	51

The values of the inclination angles of the PEG chains determined from the integrated intensity of the  $\nu_s(\text{C-O-C})$  band at  $1116\text{ cm}^{-1}$  present the same trend as the values calculated from the symmetrical  $\nu_s(\text{CH}_2)$  band at  $2853\text{ cm}^{-1}$ . Indeed, the inclination of the PEG chains on the Au and Au-NH<sub>2</sub> substrates is very close. Conversely, the inclination of the PEG chains on the hydrophobic Au-CH<sub>3</sub> substrate is much more important. Although the inclination angles of the PEG chains follow the same trend, the  $\alpha$  values present deviations depending on the absorption band used for quantitative calculations (see Tables 2 and 3). This discrepancy could come from contributions of the (CH<sub>2</sub>) and (C-C) vibrational modes present in the absorption domain of the (C-O-C) vibrational modes. The broad PM-IRRAS absorption bands of adsorbed PEG on the hydrophobic substrate may suggest that this substrate is less favorable for PEG crystallization. The narrower absorption bands observed on the PM-IRRAS spectrum of PEG adsorbed on the hydrophilic Au-NH<sub>2</sub> substrate would be characteristic of a more regular arrangement of chains. To ensure the organization of the PEG in thin films on the different model substrates, the widths at the half-height of the absorption bands in the region of  $\nu(\text{C-O-C})$  are compared in Table 4.

**Table 4.** Half-height widths of PEG absorption bands in the region of C-O-C stretching modes between  $1000\text{ cm}^{-1}$  and  $1200\text{ cm}^{-1}$ .

Wavenumbers	Assignment	Band Half-Height Width	
		Au-NH <sub>2</sub>	Au-CH <sub>3</sub>
$1146\text{ cm}^{-1}$	$\nu_a(\text{C-O-C}) + \nu(\text{C-C})$	$19\text{ cm}^{-1}$	$33\text{ cm}^{-1}$
$1116\text{ cm}^{-1}$	$\nu_s(\text{C-O-C})$	$12\text{ cm}^{-1}$	$55\text{ cm}^{-1}$
$1033\text{ cm}^{-1}$	$\nu_a(\text{C-O-C}) + \nu_s(\text{CH}_2)$	-	$28\text{ cm}^{-1}$

The widths at the half-height of the absorption bands characteristic of vibration modes of the (C-O-C) bonds of PEG are lower for the hydrophilic Au-NH<sub>2</sub> substrate than for the hydrophobic Au-CH<sub>3</sub> substrate. These narrow bands may indicate that a structured organization of PEG on these substrates is possible, more particularly on the Au-NH<sub>2</sub> substrate whose widths at half-height are lower for all the bands in this region of the spectrum. The broad absorption bands of PEG on the Au-CH<sub>3</sub> substrate indicate a decrease in the crystallinity of PEG on this hydrophobic substrate. A study of the morphology of PEG on these different model substrates would help to support these hypotheses.

#### 4.2. Surface Topology of PEG Thin Film

The morphology of PEG thin films on model substrates was characterized by AFM in contact mode. AFM pictures are presented in Figure 14.

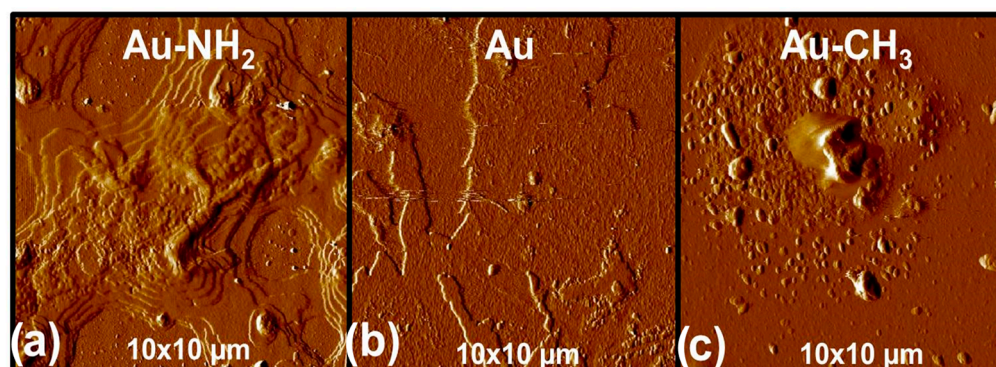


**Figure 14.** AFM pictures of the deflection signal in contact mode ( $10\ \mu\text{m} \times 10\ \mu\text{m}$ ) of PEG thin film adsorbed on (a) Au-NH<sub>2</sub> hydrophilic substrate, (b) Au gold substrate and (c) Au-CH<sub>3</sub> hydrophobic substrate.

On the Au-CH<sub>3</sub> hydrophobic substrate, the hydrophobic repulsive interfacial forces between PEG and the Au-CH<sub>3</sub> surface limit the “flat” adsorption of PEG chains. The corresponding AFM picture (Figure 14c) reveals a “dewetting”-like surface pattern of collapsed PEG chains forming chain clusters. As a consequence, the roughness is rather high, i.e.,  $R_a = 60\ \text{nm}$ . Thus, the PEG/PEG interchain interactions are favored. The value of the inclination angle ( $51^\circ$ ) is very close to the magic angle ( $54^\circ$ ) corresponding to a statistical and isotropic orientation of the transition moments ( $\cos^2\theta = 1/3$ ). Thus, it can be hypothesized that adsorption of the PEG chains on the hydrophobic substrate occurs at the statistical coil state. The surface topology of the PEG deposit on the hydrophobic surface thus explains the value of the inclination angle of the PEG chains inferred from PM-IRRAS infrared spectra and confirms the PEG amorphization. Indeed, the chains being in an unfavorable state cannot organize themselves. On the hydrophilic surface (Figure 14a), the adsorbed PEG thin film adopts a “terraced” surface topology characteristic of a lamellar stacking on the substrate associated with a high roughness value, i.e.,  $R_a = 124\ \text{nm}$ . The PEG chains are spread out on the surface, confirming the parallel orientation of the chains relative to the surface area deduced from PM-IRRAS analyses of PEG adsorbed on the Au-NH<sub>2</sub> surface. The hydrophilic nature of the Au-NH<sub>2</sub> substrate thus seems to be favorable to the crystallization of PEG chains in the form of stacked “terraces”. Moreover, the surface free energy of the Au-NH<sub>2</sub> surface is very close to that of PEG, and thus the hydrophilic graft can also explain the ability of PEG chains to crystallize on this substrate. The surface of the hydrophilic Au-NH<sub>2</sub> substrate is terminated by NH<sub>2</sub> groups, giving the substrate its hydrophilic character. Lamellar growth parallel to the substrate could then be initiated by the interactions between the PEG chain ends (OH) and NH<sub>2</sub> groups through hydrogen bonding. One can ask for the consequence of these surface topologies of PEG structures (coil state vs. lamellar stacking) in the wettability of the PEG thin film surface. Nevertheless, determination of the values of water contact angles is not possible on PEG film on Au, PEG film on Au-CH<sub>3</sub> and PEG film on Au-NH<sub>2</sub>. The reason is that a water droplet swells and solubilizes PEG chains due to the hydrophilic character of PEG. To be significant, contact angles can only be measured with droplets of a non-solvent of PEG chains. One can thus consider contact angles of nonpolar liquids (1-bromonaphtalène (surface tension =  $44.4\ \text{mJ}\cdot\text{m}^{-2}$ ) or hexadecane (surface tension =  $27.5\ \text{mJ}\cdot\text{m}^{-2}$ ), but due to their surface tension being lower (hexadecane) or quite equal (1-bromonaphtalène) to the PEG surface tension ( $43\text{--}45\ \text{mJ}\cdot\text{m}^{-2}$ ), they fully spread (contact angle  $\approx 0^\circ$ ) onto the PEG surface and are irrelevant to support PM-IRRAS or AFM analysis.

A more detailed 3D topographic representation of the PEG thin film on the hydrophilic substrate is given in Figure 15.

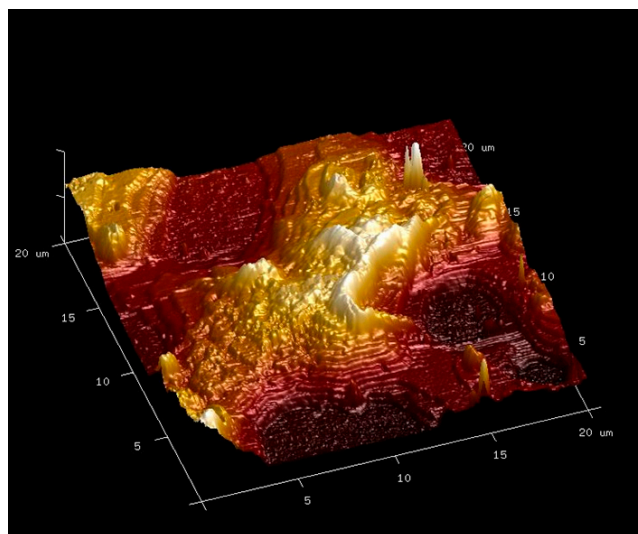


**Figure 15.** 3D AFM picture ( $20\ \mu\text{m} \times 20\ \mu\text{m}$ ) of the deflection signal in contact mode for PEG thin film spin-coated on the Au-NH<sub>2</sub> hydrophilic substrate.

The 3-dimensional representation (Figure 15) made it possible to measure the thickness of the terraces equal to approximately 20 nm. According to Yoshihara et al. [20], the length of a PEG chain containing 7 repetitive units is equal to 1.91 nm. The PEG chain with an average molar mass equal to  $2050\ \text{g}\cdot\text{mol}^{-1}$  contains 46 repetitive units and would thus be equal to 12.5 nm. The angle of inclination of the PEG chains relative to the hydrophilic Au-NH<sub>2</sub> substrate being  $25^\circ$ , the maximum height  $H$  reached by the PEG chains is calculated as  $\sin \alpha = H/L$ , with  $\alpha$  the angle of inclination of the PEG chain relative to the Au-NH<sub>2</sub> substrate,  $H$  the maximum height of the chain and  $L$  the theoretical length of an extended PEG chain. The maximum height  $H$  of a PEG chain on the hydrophilic substrate is then equal to 5.2 nm. The thickness of a terrace step would thus correspond to the stacking of approximately 4 PEG chains. These observations then make it possible to determine adsorption models of PEG chains on these different substrates.

## 5. Conclusions

Previous results showed that PEG adsorbs on substrates having a rather hydrophilic character in a way that the PEG chains spread parallel to the surface. In the case of a very hydrophilic substrate (water contact angle  $\theta = 21^\circ$ ), the adsorbed PEG chains are in a stable thermodynamic state, likewise affinity, which allows them to arrange themselves in an orderly manner (crystallization) after adsorption. Indeed, in the bulk state, PEG crystallizes in the form of very large spherulites [25] of some  $100\ \mu\text{m}$  in diameter. On Au-NH<sub>2</sub> substrates, adsorption of PEG chains is driven by surface chemistry, and PEG crystallizes in the form of stacked lamellas with a thickness equal to 20 nm. On the contrary, on a hydrophobic Au-CH<sub>3</sub> substrate, the hydrophilic repulsive interfacial forces limit the “flat” adsorption of PEG chains. Thus, the PEG/PEG interchain interactions are favored, and PEG adsorption occurs at the statistical coil state on the hydrophobic substrate. As a consequence, on the hydrophobic Au-CH<sub>3</sub> substrate, the PEG chains do not crystallize, as the surface energy of the substrate is not favorable to the development of chain/substrate interactions. Surface chemistry, and thus surface energies, significantly influence the adsorption and organization of PEG chains but also influence the crystallization morphology of PEG. Analyses of PM-IRRAS infrared spectra permit qualitative and quantitative approaches to PEG chain adsorption, supported by AFM characterization. These results thus allow the development of models of adsorption of PEG chains.

**Author Contributions:** Conceptualization, M.B. and S.B.; Methodology, D.B.; Validation, M.B., S.B. and D.B.; Formal Analysis, M.B.; Investigation, D.B.; Resources, M.B. and S.B.; Data Curation,

M.B.; Writing—Original Draft Preparation, M.B. and D.B.; Writing—Review and Editing, M.B. and S.B.; Visualization, M.B. and S.B.; Supervision, M.B. and S.B.; Project Administration, M.B. and S.B.; Funding Acquisition, M.B. All authors have read and agreed to the published version of the manuscript.

**Funding:** This research was funded by the University de Haute Alsace.

**Institutional Review Board Statement:** Not applicable.

**Data Availability Statement:** The raw data supporting the conclusions of this article will be made available by the authors upon request.

**Acknowledgments:** The authors would like to thank the Laboratory of Photochemistry and Macromolecular Engineering (LPIM, France) for access to its scientific equipment.

**Conflicts of Interest:** The authors declare no conflicts of interest.

## References

1. Kim, M.W. Surface activity and property of polyethyleneoxide (PEO) in water. *Colloids Surf. A Physicochem. Eng. Asp.* **1997**, *128*, 145–154. [[CrossRef](#)]
2. Harris, J.M.; Chess, R.B. Effect of pegylation on pharmaceuticals. *Nat. Rev. Drug Discov.* **2003**, *2*, 214–221. [[CrossRef](#)] [[PubMed](#)]
3. Pean, J.M.; Boury, F.; Venier-Julienne, M.C.; Menei, P.; Proust, J.E.; Benoit, J.P. Why does PEG 400 co-encapsulation improve NGF stability and release from PLGA biodegradable microspheres? *Pharm. Res.* **1999**, *16*, 1294–1299. [[CrossRef](#)] [[PubMed](#)]
4. Albertsson, P.A. *Partition of Cell Particles and Macromolecules*, 3rd ed.; Wiley: New York, NY, USA, 1986.
5. Kao, K.N.; Constable, F.; Michayluck, M.R.; Gamborg, O.L. Plant protoplast fusion and growth of intergeneric hybrid cells. *Planta* **1974**, *120*, 215–227. [[CrossRef](#)]
6. Pontecorvo, G. Fusing cultured mammalian cells with Polyethylene glycol. *Somat Cell Genet.* **1975**, *1*, 397–400. [[CrossRef](#)] [[PubMed](#)]
7. Buchowski, A.; van Es, T.; Palczuk, N.C.; Davis, F.F. Alteration of immunological properties of bovine serum albumin by covalent attachment of Polyethylene glycol. *J. Biol. Chem.* **1977**, *252*, 3578–3581. [[CrossRef](#)]
8. Mori, Y.; Nagoaka, S.; Takiuchi, H.; Kikuchi, T.; Noguchi, N.; Tanzawa, H.; Noishiki, Y. A new antithrombogenic material with long polyethyleneoxide chains. *Trans. Am. Soc. Art. Int. Org.* **1982**, *28*, 459–463.
9. Xiao, Y.; Yan, L.; Zhang, P.; Zhu, N.; Chen, L.; He, P. In situ Fourier transform infrared spectroscopic study of the conformational changes of high-density poly(ethylene) during the melting and crystallization processes. *J. Appl. Polym. Sci.* **2006**, *100*, 4835–4841. [[CrossRef](#)]
10. Elzein, T.; Bistac, S.; Brogly, M.; Schultz, J. PM-IRRAS spectroscopy for the characterization of polymer nanofilms: Chains conformation, anisotropy and crystallinity. *Macromol. Chem. Phys. Macromol. Symp.* **2004**, *205*, 181–190. [[CrossRef](#)]
11. Elzein, T.; Fahs, A.; Brogly, M.; Elhiri, A.; Lepoittevin, B.; Roger, P.; Planchot, V. Adsorption of Alkanethiols on Gold Surfaces: PM-IRRAS Study of the Influence of Terminal Functionality on Alkyl Chain Orientation, *J. Adhes.* **2013**, *89*, 416–432. [[CrossRef](#)]
12. Pielichowski, K.; Flejtuch, K. Differential Scanning Calorimetry Studies on Poly(ethylene Glycol) with Different Molecular Weights for Thermal Energy Storage Material. *Polym. Adv. Technol.* **2002**, *13*, 690–696. [[CrossRef](#)]
13. Li, Y.; Ma, Q.; Huang, C.; Liu, G. Crystallization of Poly(ethylene glycol) in Poly(methyl methacrylate) Networks. *Mater. Sci.* **2013**, *19*, 147–151. [[CrossRef](#)]
14. Drelich, J.; Wilbur, J.L.; Miller, J.D.; Whitesides, G.M. Contact Angles for Liquid Drops at a Model Heterogeneous Surface Consisting of Alternating and Parallel Hydrophobic/Hydrophilic Strips. *Langmuir* **1996**, *12*, 1913–1922. [[CrossRef](#)]
15. Zamlynny, V.; Lipkowski, J. Quantitative SNIPTIRS and PM IRRAS of Organic Molecules at Electrode Surfaces. In *Advances in Electrochemical Science and Engineering: Diffraction and Spectroscopic Methods in Electrochemistry*; Alkire, R.C., Kolb, D.M., Lipkowski, J., Ross, P.N., Eds.; Wiley-VCH Verlag GmbH & Co. KGaA: Weinheim, Germany, 2006; Volume 9, pp. 315–376. [[CrossRef](#)]
16. Bradley, M.S. *A New Approach to Quantitative Spectral Conversion of PM-IRRAS: Theory, Experiments, and Performance Comparisons with Conventional IRRAS*; Application Note: 51368; Thermo Fischer Scientific: Madison, WI, USA, 2008.
17. Buffeteau, T.; Desbat, B.; Turlet, J.M. Polarization Modulation FT-IR Spectroscopy of Surfaces and Ultra-thin Films: Experimental Procedure and Quantitative Analysis. *Appl. Spectroscopy* **1991**, *45*, 380–389. [[CrossRef](#)]
18. Elzein, T.; Awada, H.; Nasser-Eddine, M.; Delaite, C.; Brogly, M. A model of chain folding in Polycaprolactone-b-Polymethyl Methacrylate diblock copolymers. *Thin Solid Film* **2004**, *483*, 388–395. [[CrossRef](#)]
19. Brogly, M.; Bistac, S.; Bindel, D. Advanced surface FTIR spectroscopy analysis of poly(ethylene)-block-poly(ethylene oxide) thin film adsorbed on gold substrate. *Appl. Surf. Sci.* **2022**, *603*, 154428. [[CrossRef](#)]
20. Yoshihara, T.; Tadokoro, H.; Murahashi, S. Normal vibrations of the polymer molecules of helical conformation., IV. Polyethylene oxide and Polyethylened4 oxide. *J. Chem. Phys.* **1964**, *41*, 2902–2911. [[CrossRef](#)]
21. Pucic, I.; Jurkin, T. FTIR assessment of poly(ethylene oxide) irradiated in solid state, melt and aqueous solution. *Radiat. Phys. Chem.* **2012**, *81*, 1426–1429. [[CrossRef](#)]

22. Bergeron, C.; Perrier, E.; Potier, A.; Delmas, G. A study of the deformation, network and aging of Polyethylene oxide films by Infrared Spectroscopy and calorimetric measurements. *Int. J. Spectrosc.* **2011**, *2012*, 432046. [[CrossRef](#)]
23. Su, Y.-L.; Wang, J.; Liu, H.-Z. Melt, hydration and micellization of the PEO-PPO-PEO block copolymer studied by FTIR Spectroscopy. *J. Colloid Interface Sci.* **2002**, *251*, 417–423. [[CrossRef](#)]
24. Pereira, A.G.B.; Gouveia, R.F.; de Carvalho, G.M.; Rubira, A.F.; Muniz, E.C. Polymer blends based on PEO and starch: Miscibility and spherulite growth rate evaluated through DSC and optical microscopy. *Mater. Sci. Eng. C* **2009**, *29*, 499–504. [[CrossRef](#)]
25. Bistac, S.; Brogly, M.; Bindel, D. Crystallinity of Amphiphilic PE-b-PEG Copolymers. *Polymers* **2022**, *14*, 3639. [[CrossRef](#)] [[PubMed](#)]
26. Danolki-Veress, K.; Forrest, J.A.; Massa, M.; Pratt, A.; Williams, A. Crystal Growth Rate in Ultrathin Films of Poly(ethyleneoxide). *J. Polym. Sci. Pol. Phys.* **2001**, *39*, 2615–2621. [[CrossRef](#)]
27. Massa, M.; Danolki-Veress, K.; Forrest, J.A. Crystallization kinetics and crystal morphology in thin poly(ethylene oxide) films. *Eur. Phys. J. E* **2003**, *11*, 191–198. [[CrossRef](#)] [[PubMed](#)]
28. Vanroy, B.; Wubbenhorst, M.; Napolitano, S. Crystallization of thin polymer layers confined between absorbing walls. *ACS Macro Lett.* **2013**, *2*, 168–172. [[CrossRef](#)] [[PubMed](#)]
29. Wang, H.; Keum, J.K.; Hiltner, A.; Baer, E. Confined Crystallization of PEO in Nanolayered Films Impacting Structure and Oxygen Permeability. *Macromolecules* **2009**, *42*, 7055–7066. [[CrossRef](#)]
30. Allara, D.L.; Swalen, J.D. An infrared reflection spectroscopy study of oriented cadmium arachidate monolayer films on evaporated silver. *J. Phys. Chem.* **1982**, *86*, 2700–2704. [[CrossRef](#)]

**Disclaimer/Publisher’s Note:** The statements, opinions and data contained in all publications are solely those of the individual author(s) and contributor(s) and not of MDPI and/or the editor(s). MDPI and/or the editor(s) disclaim responsibility for any injury to people or property resulting from any ideas, methods, instructions or products referred to in the content.